JOURNAL OF SOLID STATE CHEMISTRY 112, 322–328 (1994)

# Structural Study of the Rhombohedral Fluorite-Related $R_{III}$ Phase $U_{1-y}La_yO_{2\pm x}$, $0.56 \leq y \leq 0.67$

R. M. Rojas,[1] P. Herrero, P. J. García Chain, and J. Rodriguez-Carvajal*

*Instituto de Ciencia de Materiales de Madrid, CSIC, C/Serrano 113, 28006 Madrid, Spain; and *Laboratoire Léon Brillouin (CEA-CNRS), Centre d'Etudes de Saclay, 91191 Gifsur-Yvette Cedex, France, and Institute Laue Langevin, 156X-38042 Grenoble Cedex, France*

Received August 9, 1993; in revised form December 15, 1993; accepted December 16, 1993

The structural relationships between the $R_{III}$ phase, existing in the $UO_3$–$UO_2$–$LaO_{1.5}$ system for the compositional range $U_{1-y}La_yO_{2\pm x}$ ($0.56 \leq y \leq 0.67$), and the fluorite structure have been definitely established by means of electron diffraction. The determination of the structure has been carried out using both X-ray and neutron powder diffraction. The $R_{III}$ phase constitutes a partially cation-ordered fluorite-related structure, where La and U/La layers alternate along $[111]_C$. The rhombohedral lattice, in its hexagonal setting, is related to the cubic fluorite substructure by the relations $a_H = \frac{1}{2}a_C - \frac{1}{2}b_C$, $b_H = \frac{1}{2}b_C - \frac{1}{2}c_C$, $c_H = 2(a_C + b_C + c_C)$. The space group ($R3m$), cell parameters $a_H \approx 3.9$ Å and $c_H \approx 18.9$ Å, and the refined structure show that the $R_{III}$ phase can be considered as isomorphous to the $CaUO_4$ structure. 

## INTRODUCTION

For the $UO_3$–$UO_2$–$LaO_{1.5}$ system, the existence of two fluorite-related rhombohedral phases, denoted $R_{III}$ and $R_{II}$, which transform reversibly into the high-temperature fluorite phase at about 1200°C has been reported (1). The $R$ phase was initially reported by Koshcheev and Kovba (2) who assigned to it the formula $U_3O_8 \cdot 2La_2O_3$ ($M_7O_{14}$). However, Diehl *et al.* (1, 3) indicated that the $R_{III}$ phase is formed between the limits 55 mole% $LaO_{1.5}$ and 66.7 mole% $LaO_{1.5}$ ($M_8O_{16}$), and the O : (La + U) ratio is constant at 2.00, which implies a fully occupied fluorite-type lattice (4).

Recently, we presented (5) general features relating the chemical composition analyzed by means of several techniques and geometrical characteristics of the fluorite lattice in the compositional range $U_{1-y}La_yO_{2\pm x}$ ($0.56 \leq y \leq 0.67$) which corresponds to the $R_{III}$ phase field. Using ED patterns and HREM we showed that samples quenched from 1400°C present diffuse scattering centered around Bragg reflections of the fluorite phase. This phenomenon has been discussed in terms of microdomain formation of the rhombohedral $R_{III}$ phase. This phase was obtained as a single phase when samples with these compositions were annealed at 1100°C (6). However, a detailed analysis of the crystal structure of this phase is still lacking.

On the other hand, for $U_{1-y}La_yO_{2\pm x}$ ($0.70 \leq y \leq 0.80$) a similar microdomain texture has been obtained in the fluorite high-temperature phase. In this case, microdomains have the $R_{II}$ structure and the annealing of materials results in formation of the $R_{II}$ phase as a single phase. It has been described as a superstructure $\sqrt{2}a_c \times \sqrt{2}a_c \times \sqrt{2}a_c$ of the cubic fluorite structure (7).

According to the data mentioned above, the aim of this work is to establish the structural relationships between the $R_{III}$ phase and the fluorite-type structure as deduced from electron diffraction patterns, as well as the complete determination of the structure of the $R_{III}$ phase by means of X-ray and neutron powder diffraction data.

## EXPERIMENTAL

Samples within the compositional range $U_{1-y}La_yO_{2\pm x}$ ($0.56 \leq y \leq 0.67$) were prepared as described elsewhere (5). All materials after being synthesized at 1400°C were annealed at 1100°C for 200 hr. Oxygen determination, X-ray photoelectron, and near-FT-IR spectroscopy were performed as detailed in Ref. (5). They were also chemically analyzed by using an ICP (inductive coupled plasma) method, with a Perkin-Elmer Plasma 40 emission spectrometer.

Powder X-ray diffraction patterns were recorded on a Siemens D-501 diffractometer using monochromatized $CuK_\alpha$ radiation. Diagrams were scanned by steps of 0.02° ($2\theta$) and 5-sec/step counting time. The scans were made in the range $10° \leq 2\theta \leq 100°$.

Neutron diffraction experiments were performed at several temperatures (indicated in Table 4) on the high-resolution powder diffractometer D2B, $\lambda = 1.595$ Å, at the Institute Laue-Langevin in Grenoble. We used a furnace with a vanadium resistor operating at a vacuum

[1] To whom correspondence should be addressed.



0022-4596/94 $6.00

of $pO_2$ about $10^{-4}$ atm for temperatures above room temperature. The experiment carried out at $-100$°C was performed using a standard Orange cryostat. The step size for these experiments was 0.05° in $2\theta$ and the explored angular range 10–150° ($2\theta$).

X-ray and neutron diffraction data were analyzed using the method described by Rietveld (8) with the program FULLPROF (9). In both cases, a pseudo-Voigt function was chosen to generate the shape of the diffraction peaks.

The neutron scattering lengths of the chemical elements involved are $b_{La} = 8.24$ fm, $b_U = 8.417$ fm, and $b_O = 5.805$ fm. Therefore, neutron diffraction experiments cannot discriminate directly between the ordering of La and U ions; however, oxygen ions can be very well localized. X-ray diffraction acts as a complementary technique: the atomic numbers of U, La, and O are in such a relation that U and La can clearly be distinguished and O scatters so weakly that the positions cannot be precisely determined.

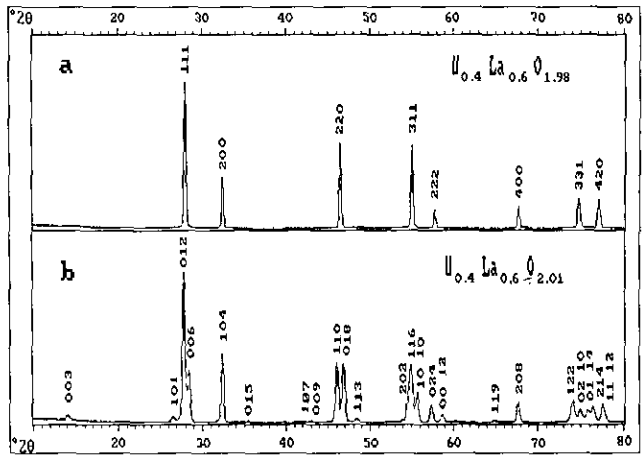


FIG. 1. X-ray diffraction patterns of the material $y = 0.60$ (a) quenched from 1400°C (fluorite phase) and (b) annealed at 1100°C ($R_{III}$ phase).

## RESULTS

The results of the chemical analysis of uranium and lanthanum indicate that there is no appreciable volatilization of the metallic elements in our samples compared to the starting nominal compositions.

Materials quenched from 1400°C showed X-ray powder patterns characteristic of the fluorite structure (space group $Fm3m$) (Fig. 1a). Cell parameters are listed in Table 1. The proposed formulation for these samples (Table 1) has been deduced from chemical analysis, oxygen content determination, X-ray photoelectron, and near-FT-IR spectroscopy, as explained in Ref. (5).

Annealing of these materials at 1100°C for 200 hr leads to the formation of the $R_{III}$ phase as a single phase, as shown in the X-ray diffraction diagrams (Fig. 1b). Cell parameters of the hexagonal cell are gathered in Table 1. In this case, the formulation has been deduced on the basis of chemical analysis results and oxygen content determination, assuming for uranium atoms the same oxidation state distribution as in materials quenched from 1400°C, that is, $U^{4+}$ and $U^{6+}$. All compositions included in this table can be expressed by the general formula

$$U^{4+}_{1-x-1.5y}U^{6+}_{x+0.5y}La^{3+}_{y}O^{2-}_{2+x}.$$

Materials with the fluorite-type structure are slightly oxygen deficient, while $R_{III}$ samples can be considered as nearly stoichiometric. What makes this possible is the increase in the relative amount of $U^{6+}$ with increasing lanthanum content.

The relationship between both structures can be estab-

TABLE 1
**Composition, Cell Parameters, and Proposed Formulation for Materials $U_{1-y}La_yO_{2\pm x}$ Quenched from 1400°C and Annealed at 1100°C**

| Lanthanum content ($y$) | Materials quenched from 1400°C | | Materials annealed at 1100°C | |
|---|---|---|---|---|
| | Formulation | Cubic cell parameter (Å) | Formulation | Hexagonal cell parameters (Å) |
| 0.56 | $U^{4+}_{0.17}U^{6+}_{0.27}La^{3+}_{0.56}O_{1.99}$ | $a_C = 5.5284(1)$ | $U^{4+}_{0.15}U^{6+}_{0.29}La^{3+}_{0.56}O_{2.01}$ | $a_H = 3.94(3)$<br>$c_H = 18.81(5)$ |
| 0.60 | $U^{4+}_{0.12}U^{6+}_{0.28}La^{3+}_{0.60}O_{1.98}$ | $a_C = 5.5385(2)$ | $U^{4+}_{0.09}U^{6+}_{0.31}La^{3+}_{0.60}O_{2.01}$ | $a_H = 3.9453(1)$<br>$c_H = 18.8943(8)$ |
| 0.64 | $U^{4+}_{0.07}U^{6+}_{0.29}La^{3+}_{0.64}O_{1.97}$ | $a_C = 5.5477(4)$ | $U^{4+}_{0.04}U^{6+}_{0.32}La^{3+}_{0.64}O_{2.00}$ | $a_H = 3.93(3)$<br>$c_H = 18.94(1)$ |
| 0.67 | $U^{4+}_{0.05}U^{6+}_{0.28}La^{3+}_{0.67}O_{1.95}$ | $a_C = 5.5533(4)$ | $U^{4+}_{0.01}U^{6+}_{0.32}La^{3+}_{0.67}O_{1.99}$ | $a_H = 3.94(1)$<br>$c_H = 18.97(2)$ |

*Note.* Estimated error in the oxygen content determination, ±0.01.

lished from the corresponding electron diffraction patterns. Figure 2 shows the selected area for electron diffraction patterns of the material $y = 0.60$ corresponding to the $[1\bar{1}0]_C$, $[111]_C$, $[121]_C$, and $[332]_C$ orientations of the fluorite cell (left-hand side) which are parallel to the $[100]_H$ and $[001]_H$ projections of the hexagonal cell of the $R_{III}$ phase and to the $[001]_R$ and $[0\bar{1}1]_R$ of the same phase in the rhombohedral setting (right-hand side) (subscripts C, H, and R refer to cubic, hexagonal, and rhombohedral cells, respectively). The reader can easily verify, from Fig. 2, that the relations between the reciprocal (direct) cells of the cubic-fluorite structure and the reciprocal (direct) cells of the $R_{III}$ phase are

Hexagonal setting:

$$\mathbf{a}_H^* = 4/3\mathbf{a}_C^* - 2/3\mathbf{b}_C^* - 2/3\mathbf{c}_C^*, \qquad \mathbf{a}_H = 1/2\mathbf{a}_C - 1/2\mathbf{b}_C$$

$$\mathbf{b}_H^* = 2/3\mathbf{a}_C^* + 2/3\mathbf{b}_C^* - 4/3\mathbf{c}_C^*, \qquad \mathbf{b}_H = 1/2\mathbf{b}_C - 1/2\mathbf{c}_C$$

$$\mathbf{c}_H^* = 1/6(\mathbf{a}_C^* + \mathbf{b}_C^* + \mathbf{c}_C^*), \qquad \mathbf{c}_H = 2(\mathbf{a}_C + \mathbf{b}_C + \mathbf{c}_C)$$

Rhombohedral setting:

$$\mathbf{a}_R^* = 1/2\mathbf{a}_C^* - 1/2\mathbf{b}_C^* + 3/2\mathbf{c}_C^*, \qquad \mathbf{a}_R = 1/2\mathbf{a}_C + 1/2\mathbf{b}_C + \mathbf{c}_C$$

$$\mathbf{b}_R^* = 3/2\mathbf{a}_C^* - 1/2\mathbf{b}_C^* - 1/2\mathbf{c}_C^*, \qquad \mathbf{b}_R = \mathbf{a}_C + 1/2\mathbf{b}_C + 1/2\mathbf{c}_C$$

$$\mathbf{c}_R^* = -1/2\mathbf{a}_C^* + 3/2\mathbf{b}_C^* - 1/2\mathbf{c}_C^*, \qquad \mathbf{c}_R = 1/2\mathbf{a}_C + \mathbf{b}_C + 1/2\mathbf{c}_C.$$

From these relations one may obtain the dimensions of the direct cell parameters: $a_H \approx \sqrt{1/2}a_C$, $c_H \approx 2\sqrt{3}a_C$, $a_R \approx \sqrt{3/2}\,a_C$, and $\alpha \approx 33°$. The calculated values are in good agreement with those obtained from X-ray powder diffraction data: $a_H = 3.9453(1)$ Å and $c_H = 18.8943(8)$ Å; $a_R = 6.697(5)$ Å and $\alpha_R = 34.26°$.

Figure 3a schematizes the relationship between the cubic and the hexagonal cells in the reciprocal space, while Fig. 3b shows the relation between both direct cells.

## STRUCTURE ANALYSIS AND REFINEMENT

According to the above indicated data, the $R_{III}$ phase can be considered as a superstructure of the fluorite cell, and its formation is explained on the basis of an ordering in the cationic sublattice. A model that would account for the fluorite $\leftrightarrow$ $R_{III}$ transformation has been outlined in Fig. 4, in which only the cationic arrangement has been represented. It can be derived from the $UO_2$ cell, by an ordered substitution of uranium atoms for lanthanum atoms. The corresponding compositions depending on the La content are indicated. The resultant cationic sublattice is then built up by a sequence of La and mixed U/La layers that alternates in an ordered way along the $[111]_C$ direction. This model closely resembles the $CaUO_4$ structure (space group $R\bar{3}m$) (10, 11), and therefore the structure analysis on the material $y = 0.60$, that may be formulated as $La_{1.20}U_{0.80}O_{4.02}$, was made by assuming the same space group.

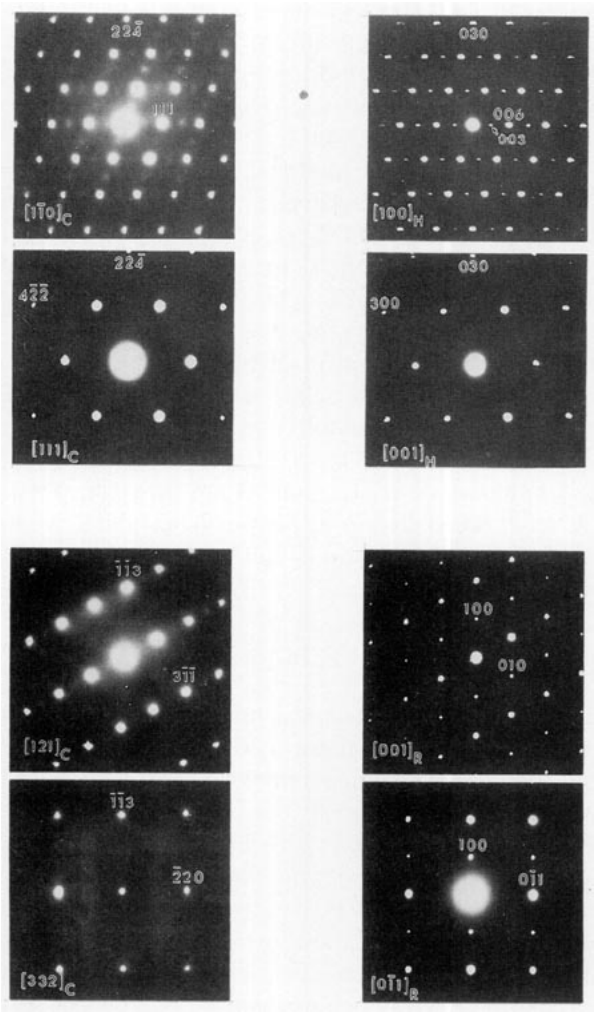


FIG. 2. Selected area diffraction patterns of the material $y = 0.60$: (left) quenched from 1400°C (fluorite phase); (right) annealed at 1100°C ($R_{III}$ phase). Zone axes are indicated.

X-ray diffraction confirms (see Fig. 5) unambiguously the cation ordering postulated. The structure factor for allowed reflections in space group $R\bar{3}m$, neglecting temperature factors, can be written for the $R_{III}$ phase as:

$$F(hkl) = 3[f_{3a} + (-1)^l f_{3b} + 2f_{ox}\{\cos(2\pi z_1 l) + \cos(2\pi z_2 l)\}] \approx 3[f_{3a} + (-1)^l f_{3b}],$$

where $f_w$ ($W = 3a, 3b$) stands for the scattering factor of the average atom occupying the Wyckoff position $W$, $f_{ox}$ is the scattering factor of oxygen, and $z_1$ and $z_2$ correspond to the $z$ coordinates of the two positions 6c occupied by oxygen atoms. A complete disordered structure produces nearly zero intensities for reflections having an odd $l$ in-

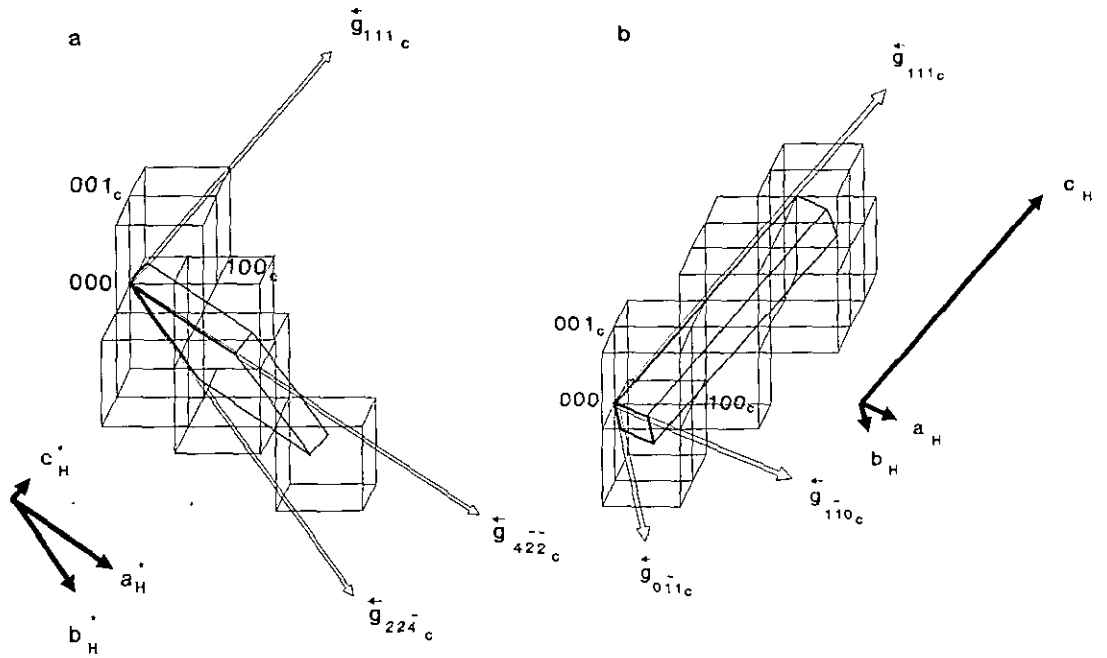


FIG. 3. Representation of the $R_{III}$ hexagonal lattice showing the relative orientations with respect to the cubic fluorite cell: (a) reciprocal space; (b) real space.

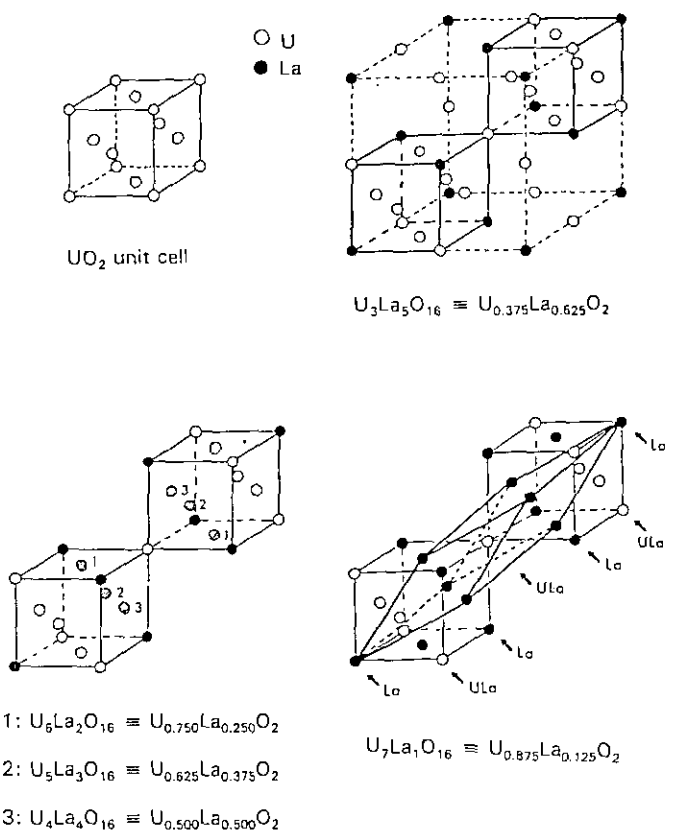


FIG. 4. Schematic model accounting for the fluorite → $R_{III}$ transformation; only the cationic sublattice is shown. Compositions are referred to the two indicated cubes.

dex. This is shown in the inset of Fig. 5, where reflections (003) and (101) are clearly seen and there is no intensity calculated with the disordered model. The refinement of the occupation of the two sites establishes that there are nearly no U atoms in the 3*a* position, within an experimental error estimated in $5\sigma$, where $\sigma$ is the least-square standard deviation. The X-ray diffraction pattern is affected by some systematic errors because the overall temperature factor is negative; however, this has a minor influence on the value of the cation distribution parameters.

Although the information given by X-ray diffraction data allows the localization of the heavy atoms, a more accurate determination of the light atom positions can be achieved from neutron powder diffraction data. The observed and calculated neutron diffraction patterns are shown in Fig. 6. Moreover, the *M*–O distances obtained from neutron diffraction provide an independent (and indirect) test of the cation distribution: shorter *M*–O distances are indicative of the presence of smaller $U^{5+}$ ions. In Table 2 crystallographic data and fractional atomic coordinates obtained from neutron Rietveld refinement are given; in Table 3 the most significant interatomic distances and angles are presented.

Neutron diffraction patterns were performed at temperatures gathered in Table 4, in which cell parameter values at each temperature are shown. From these values, thermal expansion coefficients for $a_H$ and $c_H$ ($\alpha_i = 1/a_i \cdot da_i/dT$; $i = a_H$ and $c_H$) have been calculated. They show a

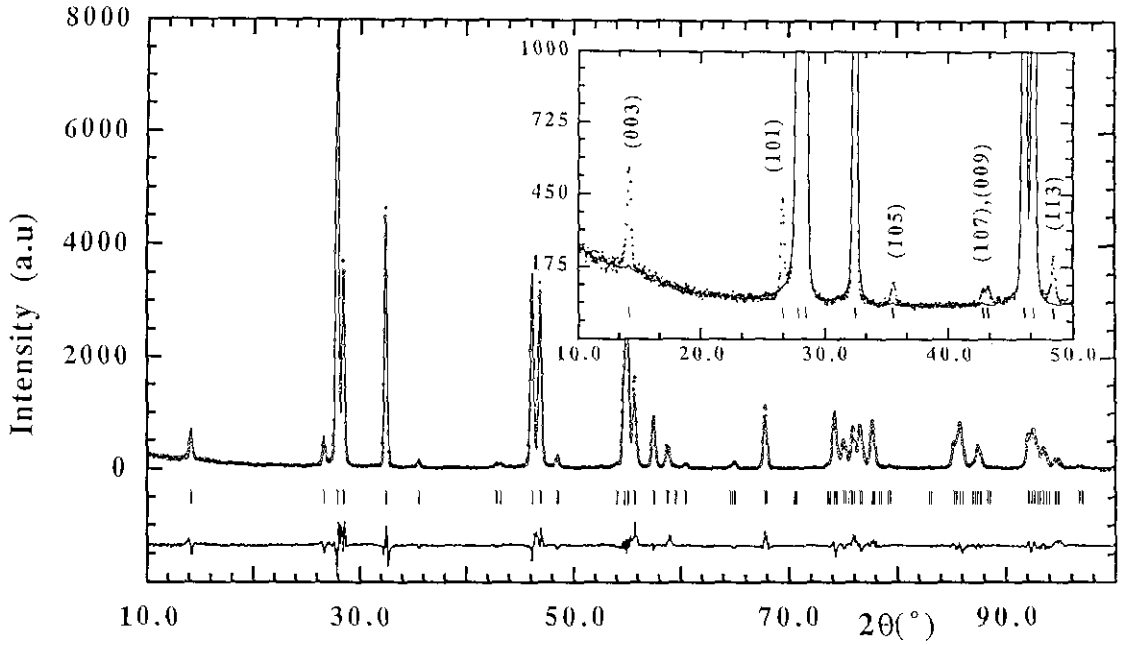


FIG. 5. Calculated (—) and experimental (O) X-ray diffraction profiles for material $y = 0.60$ annealed at 1100°C.

variation with temperature that can be fitted to a second-order polynomial expression $\alpha = C_0 + C_1T + C_2T^2$; the equations relating $a_H$ and $c_H$ values with temperature are

$$a_H(t) = a_H(T_0)(1 + 1.6789 \times 10^{-5}T + 5.2284 \times 10^{-9}T^2 + 5.1914 \times 10^{-12} \times T^3)$$

$$c_H(T) = c_H(T_0)(1 + 1.6518 \times 10^{-5}T + 1.8284 \times 10^{-9}T^2 + 1.6256 \times 10^{-12} \times T^3),$$

where $a_H(T_0)$ and $c_H(T_0)$ stand for cell parameters at $-100$°C.

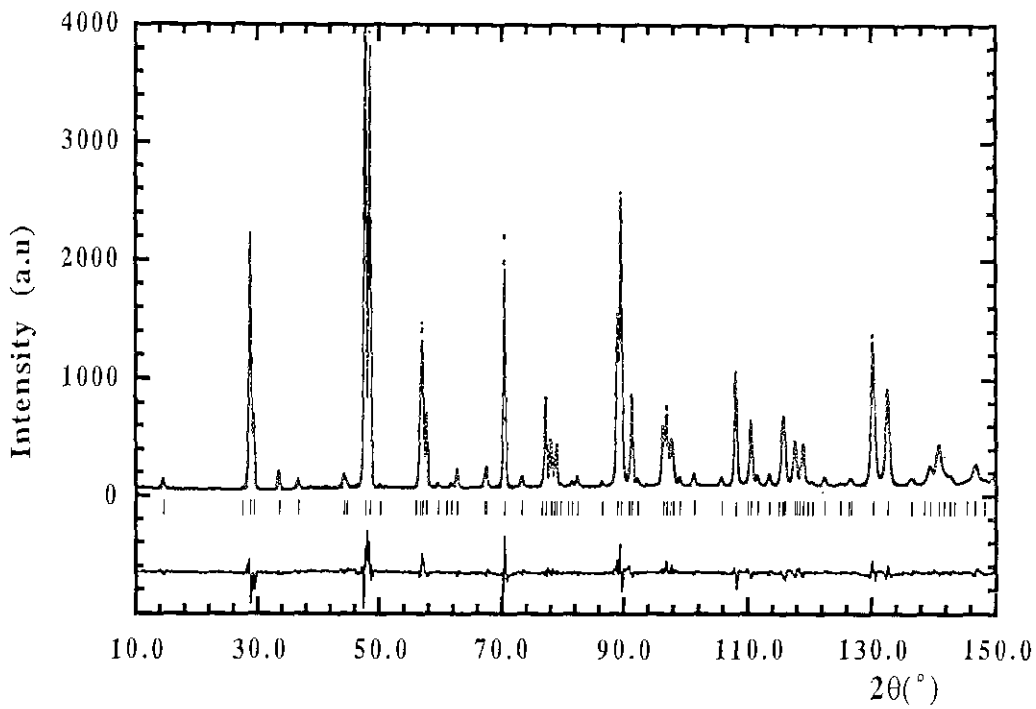


FIG. 6. Calculated (—) and experimental (O) neutron diffraction profiles for material $y = 0.60$ annealed at 1100°C.

TABLE 2
Neutron Data Collection, Structural Parameters, and Rietveld Refinement Data for $La_{1.20}U_{0.80}O_{4.02}$ ($R_{III}$ Phase)

| | | | |
|---|---|---|---|
| Scan range | 10–150° $2\theta$ | No. of reflections | 86 |
| Temperature | −100°C | Structural parameters | 10 |
| | | Profile parameters | 16 |
| | | No. of fitted parameters | 26 |

Space group $R\bar{3}m$ (Hexagonal setting)
$a_H$ = 3.94275(5) Å $\alpha$ = 90°
$b_H$ = 3.94275(5) Å $\beta$ = 90°
$c_H$ = 18.8789(3) Å $\gamma$ = 120°
$V$ = 254.160 Å$^3$ $Z$ = 3

Background corrected $R$ factors (%)
$R_p$ = 11.1
$R_{wp}$ = 12.5
$R_{exp}$ = 3.68
$X$ = 11.5
$R_{Bragg}$ = 4.38

| Atom | $x$ | $y$ | $z$ | Anisotropic temperature factor ($\times 10^4$) $\beta_{11} = \beta_{22}$ | $\beta_{33}$ | $\beta_{12} = \frac{1}{2}\beta_{11}$ | P.F. |
|---|---|---|---|---|---|---|---|
| La1 | 0.0000 | 0.0000 | 0.0000 | 76.90 | 2.50 | 38.30 | 0.5000 |
| La2/U | 0.0000 | 0.0000 | 0.5000 | 60.52 | 2.60 | 30.26 | 0.1000/0.4000 |
| O1 | 0.0000 | 0.0000 | 0.1334(6) | 365.70 | 8.40 | 183.00 | 1.0000 |
| O2 | 0.0000 | 0.0000 | 0.3847(7) | 181.80 | 15.00 | 91.00 | 1.0000 |

## DISCUSSION OF THE STRUCTURE

From the above results, it follows that the rhombohedral $R_{III}$ phase can be regarded as a deformed fluorite-type structure and can be derived from it by a slight compression along one of the threefold axes. Both La and U atoms are eightfold coordinated and the structure can be described as built up by interlocked $LaO_8$ and (U/La)$O_8$ polyhedra, where La and U/La mixed layers alternate along the $c$ axis of the hexagonal cell, parallel to $[111]_C$ (Fig. 7). Each lanthanum atom La(1) in an unmixed layer is bonded to two and six oxygen atoms at 2.5184(4) and 2.4744(7) Å, respectively, resulting in a slightly distorted cube (Fig. 8a). These distances are within the values reported for A–$La_2O_3$ (12) and for $La_6UO_{12}$ (13). However, U/La situated in the mixed layer is bonded to six and two oxygen atoms at 2.3615(2) and 2.1767(3) Å, re-

TABLE 3
Selected Interatomic Distances (Å) and Angles (Degrees)

| Atoms | Distances (Å) or Angles (degrees) |
|---|---|
| La(11)–2O(11) | 2.5184(4) |
| –6O(23) | 2.4744(7) |
| O(11)–La(11)–O(12) | 180.000 |
| O(11)–La(11)–O(23) | 66.912(5) |
| O(11)–La(11)–O(26) | 113.088(5) |
| U/La(21)–2O(21) | 2.1767(3) |
| –6O(14) | 2.3615(2) |
| O(21)–U/La(21)–O(22) | 180.000 |
| O(21)–U/La(21)–O(14) | 105.440(3) |
| O(21)–U/La(21)–O(15) | 74.561(3) |

*Note.* Symmetry code: La(11), O, O, O; O(11), O, O, $z$; O(12), O, O, $1 - z$; O(23), $\frac{1}{3}, \frac{2}{3}, z' - \frac{1}{3}$; O(26), $\frac{2}{3}, \frac{1}{3}, z' - \frac{2}{3}$; U/La(21), O, O, $\frac{1}{2}$; O(21), O, O, $z'$; O(14), $\frac{1}{3}, \frac{2}{3}, \frac{2}{3} - z$; O(22), O, O, $1 - z'$; O(15), $\frac{2}{3}, \frac{1}{3}, \frac{1}{3} + z$.

TABLE 4
Cell Parameter Values at Different Temperatures, from Neutron Diffraction Patterns, and Thermal Expansion Coefficients for Material with Composition $y = 0.60$

| Temperature (°C) | Cell parameters (Å) $a_H$ | $c_H$ | $\alpha_i \times 10^5$(°C$^{-1}$) $\alpha_{a_H}$ | $\alpha_{c_H}$ |
|---|---|---|---|---|
| −100 | 3.9427(5) | 18.878(3) | 1.6326 | 1.1485 |
| 460 | 3.9713(8) | 18.989(5) | 2.0198 | 1.2808 |
| 550 | 3.9768(9) | 19.008(6) | 2.1308 | 1.3224 |
| 650 | 3.9840(1) | 19.032(6) | 2.2411 | 1.3460 |
| 750 | 3.9920(1) | 19.056(7) | 2.3658 | 1.3959 |
| 850 | 4.0010(1) | 19.083(9) | 2.4944 | 1.3741 |
| 930 | 4.0090(1) | 19.104(9) | | |

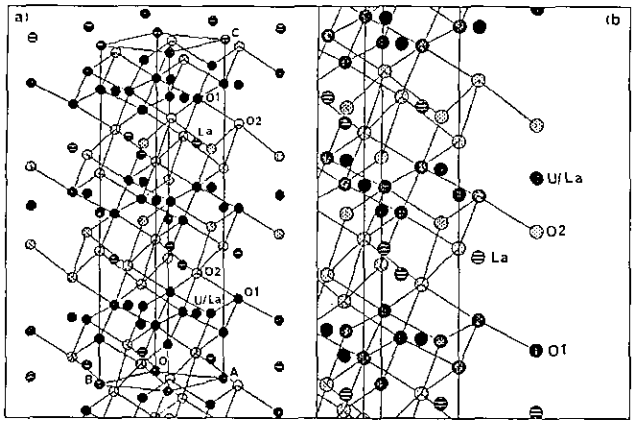


FIG. 7. Perspective view of the structure of material $y = 0.60$: (a) unit cell picture; (b) enlarged area in which coordination polyhedra and packing can be seen.

spectively; the coordination polyhedra in this case can be regarded as a higher distorted cube (Fig. 8b). However, the U/La–O(21) distance does not provide direct evidence for the existence of an uranyl group $UO_2^{2+}$, as has been claimed to exist in $CaUO_4$ (10). The most representative bond distances and angles are given in Table 3.

According to the results presented in Table 1, in these materials a high proportion of $U^{6+}$, which can hardly be accommodated in a cubic surrounding, exists. At high temperature, thermal excitations of oxygen atoms tend to establish a diffuse regime—at 1600°C the oxygen sublattices in these types of materials can be considered as a quasi-liquid (14)–and it would provoke a dynamical distribution of oxygen atoms around the fluorite equilibrium positions. Therefore, the fluorite-type structure can be obtained on materials quenched from 1400°C, although microdomains of the $R_{III}$ phase are always present. However, at temperatures below 1200°C, a readjustment of the oxygen atoms takes place, resulting in a distortion of the coordination polyhedra around $U^{6+}$ in an ordered way. The statistical distribution of $U^{4+}/U^{6+}/La^{3+}$ in the mixed layers, which alternate with unmixed La layers along $[111]_C$, would account for the compositional range of the $R_{III}$ phase, that can be regarded as a partially cation-ordered related fluorite structure.

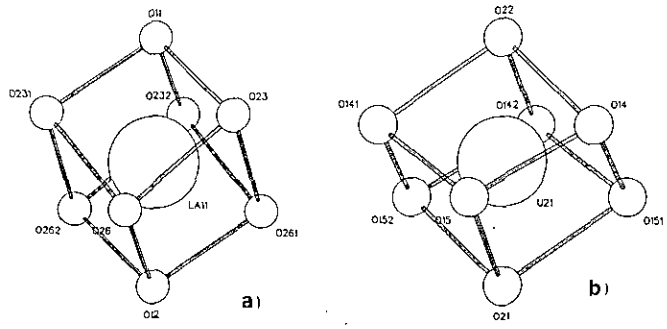


FIG. 8. Coordination polyhedra around (a) La atom and (b) U/La atoms. Atom labels are the same as those in Table 3.

## ACKNOWLEDGMENTS

We thank Professor F. Hernández Cano for his valuable comments. We acknowledge Mr. Garcia Delgado for the performance of the electron microscopy and Mr. Ropero for technical assistance. We are also indebted to the ILL staff for help in the use of the ancillary equipment and the allocation of beam time. This work has been supported by CICYT Project MAT 89/0567.

## REFERENCES

1. H. G. Diehl and C. Keller, *J. Solid State Chem.* **3,** 621 (1971).
2. G. G. Koshcheev and L. M. Kovba, *Inorg.Mater.* **2,** 1070 (1966).
3. C. Keller, *in* "MTP International Review of Science" (K. W. Bagnall Ed.), Vol. 7, Ser. 2, p. 12. Butterworths, London, 1975.
4. D. J. M. Bevan and E. Summerville, "Handbook of the Physics and Chemistry of Rare Earth" (K. A. Gschneider, Jr., and L. Eyring, Eds.), Vol. 3, Chap. 28, p. 448. North-Holland, Amsterdam, 1979.
5. P. Herrero, P. Garcia-Chain, and R. M. Rojas, *J. Solid State Chem.* **87,** 331 (1990).
6. R. M. Rojas, P. Garcia-Chain, and P. Herrero, *Solid State Ionics* **44,** 263 (1991).
7. P. Garcia-Chain, R. M. Rojas, P. Herrero, and J. R. Günter, *J. Solid State Chem.* **108,** 236 (1994).
8. H. M. Rietveld, *J. Appl. Crystallogr.* **15,** 430 (1982).
9. J. Rodriguez-Carvajal, FULLPROF. ILL, Grenoble, France, unpublished, 1991.
10. W. H. Zachariasen, *Acta Crystallogr.* **1,** 281 (1948).
11. A. Prodan and F. W. Boswell, *Acta Crystallogr. Sect. B* **42,** 141 (1986).
12. B. G. Hyde and S. Andersson, "Inorganic Crystal Structures," Chap. V, p. 137. Wiley, New York, 1989.
13. Y. Hinatsu, N. Masaki, and T. Fujino, *J. Solid State Chem.* **73,** 567 (1988).
14. R. Wallenberg, R. Withers, D. J. M. Bevan, J. G. Thompson, P. Barlow, and B. G. Hyde, *J. Less-Common Met.* **156,** 1 (1989).